Molecular Therapy
Nucleic Acids
Original Article

Design, pharmacology, and toxicology of a novel chemically modified siRNA targeting hepatic angiotensinogen

Ze-Ao Huang,[1,2] Guang-Shen Ji,[1,2] Shuo Yang,[1,2] Yang Yang,[1] Yu-Cheng Wu,[1] Zhi-Kang Tian,[1] and Geng-Shen Song[1]

[1]Beijing Youcare Kechuang Pharmaceutical Technology Co., Ltd., Kechuang 7th Street, BDA, Beijing 100176, China

Angiotensinogen (AGT) is the precursor of angiotensin II, a potent vasopressor in the renin-angiotensin-aldosterone system. Small interfering RNAs (siRNAs) targeting hepatic AGT can lower blood pressure in hypertension patients by reducing AGT levels, with effects lasting over 6 months. Existing siRNA molecules are effective, but novel ones with better inhibitory activity and longer duration periods may be developed. In this study, we demonstrated an entire development process for a novel siRNA targeting hepatic AGT. Through the proper combination of bioinformatic on-target/off-target screening on sequences, chemical modification patterns optimization, and liver-targeting delivery ligands conjugation, we have successfully developed several promising siRNAs with equivalent or better inhibitory activity, duration of effect, and safety profile compared with previously reported siRNA. Moreover, our comprehensive analysis has elucidated the correlation between the efficacy and free energy of siRNAs. Currently, there exists no reliable model capable of precisely predicting the activity and off-target risk associated with fully modified siRNAs. Therefore, the implementation of efficient screening procedures is of utmost importance during the development of siRNA candidates. This study presents a meticulous and valuable reference for the development of potent and safe siRNAs on other targets.

INTRODUCTION

Hypertension is a serious and chronic medical condition that impacts 33% of adults aged 30–79 years worldwide.[1] It has become the primary risk factor for mortality around the world since hypertension could increase the mortality rates associated with cardiovascular and kidney disease.[2] However, merely around one-fifth of individuals with hypertension have their blood pressure under control.[1] The high incidence of uncontrolled hypertension can be predominantly attributed to low adherence to treatment,[3] as well as negative feedback of the renin-angiotensin-aldosterone system (RAAS), which could counteract the efficacy of anti-hypertensive drugs.[4–6] Angiotensinogen (AGT) is a plasma glycoprotein mainly produced by the liver.[7] As an important protein in the RAAS system and the source of all angiotensin peptides, the blockade of AGT production, whether through antisense oligonucleotides or small interfering RNAs (siRNAs),[8,9] can effectively impede the activity of RAAS. This, in return, leads to a reduction of blood pressure. Zilebesiran, a siRNA that targets *AGT*, is currently in phase II clinical trial[10] and has shown its capacity to lower blood pressure for up to 6 months following a single subcutaneous administration. This finding suggests that *AGT*-targeting siRNAs could serve as an effective antihypertensive treatment.[11]

Although Zilebesiran has already shown excellent efficacy and safety profiles,[10,11] we believe that in the future, a large number of hypertensive patients will require multiple options for these promising siRNA-based therapies.[1] Moreover, the full potential of siRNAs remains untapped, which motivates us to strive to improve the efficacy of *AGT*-targeting siRNAs.

Actually, the efficacy of siRNAs is influenced by many factors, such as sequence composition, chemical modification patterns applied to them, and delivery systems used for their administration.[12,13] Based on Watson-Crick base pairing principles, it is feasible to design thousands of distinct siRNA sequences that target a single mRNA sequence. However, only a handful of these sequences possess sufficient potency to be utilized in therapeutic applications. Currently, accurately predicting the efficacy of siRNAs based on their sequence composition remains fraught with numerous challenges.[14] Consequently, screening a large number of siRNAs is essential to identify highly potent sequences. Chemical modification represents another pivotal factor that affects both the potency and durability of siRNAs.[13] A variety of nucleotide modifications can be introduced to siRNAs, and the distribution of these modifications along the sequences can be regarded as modification patterns. We found that different sequences exhibit distinct modification preferences, further complicating the screening process. Additionally, the delivery system

Received 20 December 2024; accepted 14 April 2025;
https://doi.org/10.1016/j.omtn.2025.102542.

[2]These authors contributed equally

Correspondence: Geng-Shen Song, Beijing Youcare Kechuang Pharmaceutical Technology Co., Ltd., Kechuang 7th Street, BDA, Beijing 100176, China.
E-mail: songgengshen@youcareyk.com

A

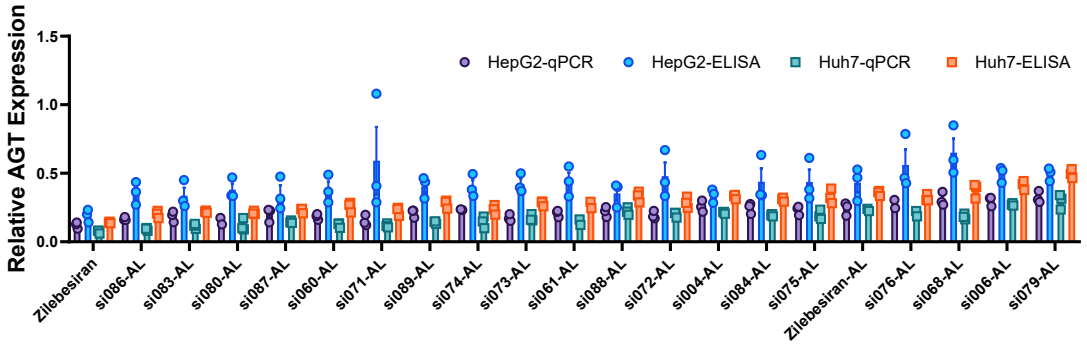

B

Name	IC_{50} / pM	
	HepG2	Huh7
si060-AL	2.25	2.26
si061-AL	6.74	2.18
si071-AL	4.29	1.05
si072-AL	9.16	2.60
si073-AL	7.16	1.91
si080-AL	6.68	2.61
si083-AL	5.10	3.39
si086-AL	2.98	2.83
si087-AL	5.06	2.26
si089-AL	7.16	6.25
Zilebesiran-AL	9.98	6.60

C

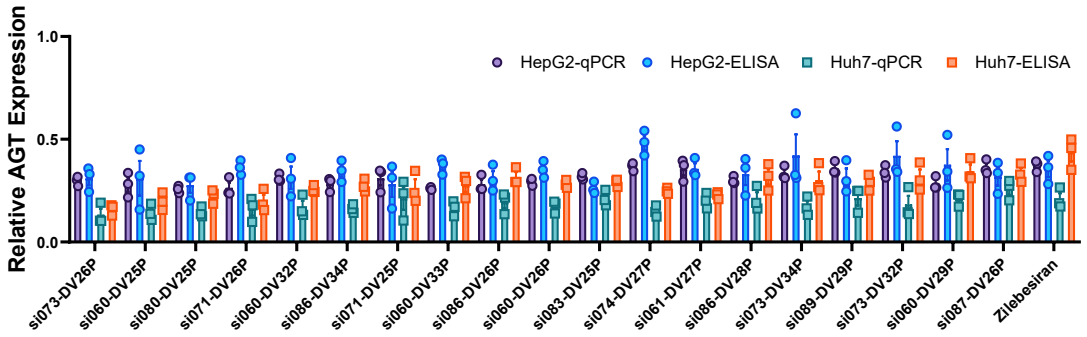

D

Name	IC_{50} / pM		Name	IC_{50} / pM	
	HepG2	Huh7		HepG2	Huh7
si060-DV25P	10.53	2.03	**si086-DV26P**	14.57	1.49
si060-DV29P	15.84	4.00	si087-DV26P	12.84	3.71
si060-DV32P	4.71	1.98	**si089-DV29P**	3.30	1.83
si061-DV27P	2.86	4.17	**si097-DV29P**	11.21	1.95
si071-DV25P	1.88	2.06	**si098-DV29P**	8.57	1.07
si071-DV26P	2.64	1.11	**si099-DV29P**	15.39	3.47
si073-DV26P	7.81	3.47	si100-DV29P	23.16	15.00
si074-DV27P	3.57	2.02	si101-DV29P	46.24	4.41
si080-DV25P	2.16	2.08	si102-DV29P	61.50	15.08
si083-DV25P	3.53	1.77	si103-DV29P	30.60	5.76
Zilebesiran	17.27	3.09	Zilebesiran	17.27	3.09

(legend on next page)

plays a critical role in siRNA efficacy and accumulation in target tissues. N-Acetylgalactosamine (GalNAc) as the ligand for the hepatocyte-specific asialoglycoprotein receptor (ASGPR) is widely used for liver-targeted siRNA delivery.[15–17] This approach has led to the successful approval of inclisiran, a siRNA developed by Alnylam targeting liver proprotein convertase subtilisin/kexin type 9 (PCSK9) to reduce plasma low-density lipoprotein cholesterol (LDL-C) levels. Since AGT is primarily liver-produced, GalNAc-based delivery is also highly effective for siRNAs targeting its gene.

To the best of our knowledge, there is currently no comprehensive systematic strategy describing the process for identifying a promising siRNA candidate. In this report, we demonstrated that an appropriate combination of sequence composition, modification patterns, and delivery systems can further enhance the efficacy and persistence of siRNA targeting *AGT* in diverse animal models. We investigated the relationship between inhibition efficacy and various features of siRNA sequences. Additionally, we evaluated the safety profiles for these siRNAs and discussed their toxicity and off-target effects. The promising siRNA candidates presented in this report have shown sufficient potency and acceptable safety in pre-clinical studies, enabling their potential application in clinical trials for antihypertensive therapy.

RESULTS

Sequences design and *in vitro* inhibition of *AGT* siRNA

A total of 96 siRNAs, which target the *AGT* mRNA with distinct sequences and are characterized by alternating 2′-F/2′-MOE modifications, were designed and synthesized. Each siRNA's sequence number is marked with "AL" (as depicted in Figures S1 and S2). The "AL" design was used to improve the stability of the siRNAs, thus circumventing potential uncertainty results stemming from the degradation of unmodified sequences. *In vitro* qPCR screening was performed at 70 pM and 50 pM in HepG2 and Huh7 cell lines, respectively (Figure S2). Nineteen siRNAs were selected from the aforementioned 96 siRNAs because of their relatively high efficacy in suppressing the expression of *AGT* mRNA. Subsequently, their protein knockdown efficiencies were also evaluated using ELISA (Figure 1A). Among them, 10 siRNAs outperformed others in both cell lines. At 48 h post-transfection, they achieved over 80% knockdown of mRNA and over 50% knockdown of protein. Moreover, their calculated IC_{50} values were in the sub-nanomolar range, indicating efficient knockdown even at low concentrations (Figure 1B; for the dose-response curves, refer to Figures S3 and S4).

Based on sequences of the 10 potent siRNAs presented in Figure 1B, we designed 75 siRNAs with distinct modification patterns. These siRNAs were named according to design variations (DV, as shown in Figure S1). Compared to AL design, DV designs reduced the number of 2′-F modifications and rearranged the modification positions with the aim of enhancing the efficacy and stability of the siRNAs. Additionally, all of these siRNAs incorporated a 5′-(*E*)-VP modification at the 5′ end of antisense strands to further boost the efficacy of the siRNAs.[18] To distinguish them, the letter "P" was added to their names, for example, DV29P. Then, another round of *in vitro* qPCR screening was carried out at a concentration of 20 pM in HepG2 and 15 pM in Huh7 cell lines, respectively (Figure S5). As a result, 19 highly potent siRNAs were selected from the aforementioned 75 siRNAs because of their relatively higher efficacy in suppressing the expression of *AGT* mRNA (Figure 1C). Subsequently, 13 potent siRNAs were selected from the aforementioned 19 siRNAs, and their IC_{50} values were evaluated in both HepG2 and Huh7 cell lines (Figure 1D).

Notably, while si060-DV25P and si086-DV34P showed excellent efficacy in these cell lines (IC_{50} in Huh7: 2.03 pM and 2.94 pM, respectively), they posed potential risks on both efficacy and safety in cynomolgus monkeys. The former had a seed-region mismatch with cynomolgus monkey *AGT* mRNA, and the latter had the most potential off-target genes predicted *in silico*. Given that cynomolgus monkeys are commonly used for pre-clinical efficacy and safety proof-of-concept (POC) studies of human-mRNA-targeting siRNAs, we additionally designed and synthesized seven new siRNAs to mitigate these potential risks: six (si097–si102) based on si060-DV25P and one (si103) based on si086-DV34P. These seven new siRNAs, combined with the 13 previously identified potent siRNAs, were tested using qPCR to generate dose-response curves (Figures 1D and S6–S9). Ultimately, 13 siRNAs were selected based on their *AGT* knockdown efficiency and IC_{50} values (Figure 1D, names in bold) and further investigated for off-target effects.

In silico off-target analysis and qPCR validation

Safety is vital for siRNA therapies. Research has suggested the hepatotoxicity of siRNAs is relevant to the miRNA-like off-target effects[19]; thus, evaluation of off-target effects on the aforementioned 13 potent siRNAs before *in vivo* toxicity studies were conducted to filter out highly toxic siRNAs. To investigate the miRNA-like off-target effects of *AGT* siRNA candidates, we performed a BLAST search for antisense siRNA sequences to identify mRNA with similar sequences in the human RefSeq RNA library. The results showed potential off-target genes with no more than one mismatch at the seed region of the antisense strand. Potential off-target genes were detected for all siRNA candidates except si061-DV27P. Subsequently, the knockdown efficiency of candidate siRNAs on these potential

Figure 1. Screening of AGT siRNA *in vitro*

(A) Nineteen potent AGT candidate siRNAs were selected in primary qPCR test in HepG2 at 70 pM and in Huh7 cell line at 50 pM and tested for protein knockdown. $n = 3$ for each group. Group means ± SEM are shown. siRNAs are ordered by efficacy. (B) Half maximal inhibitory concentration (IC_{50}) for potent candidate siRNAs in HepG2 cell line and Huh7 cell line. siRNAs were tested in 4-fold serial dilution to determine IC_{50} values for each sequence. All calculated IC_{50} were in the sub-nanomolar range. $n = 1$ for each group. (C) Second round of siRNA screening in HepG2 at 20 pM and in Huh7 cell line at 15 pM. $n = 3$ for each group. Group means ± SEM are shown. siRNAs are ordered by efficacy. (D) IC_{50} for potent candidate siRNAs in HepG2 and Huh7 cell line. All calculated IC_{50} were in the sub-nanomolar range. $n = 1$ for each group.

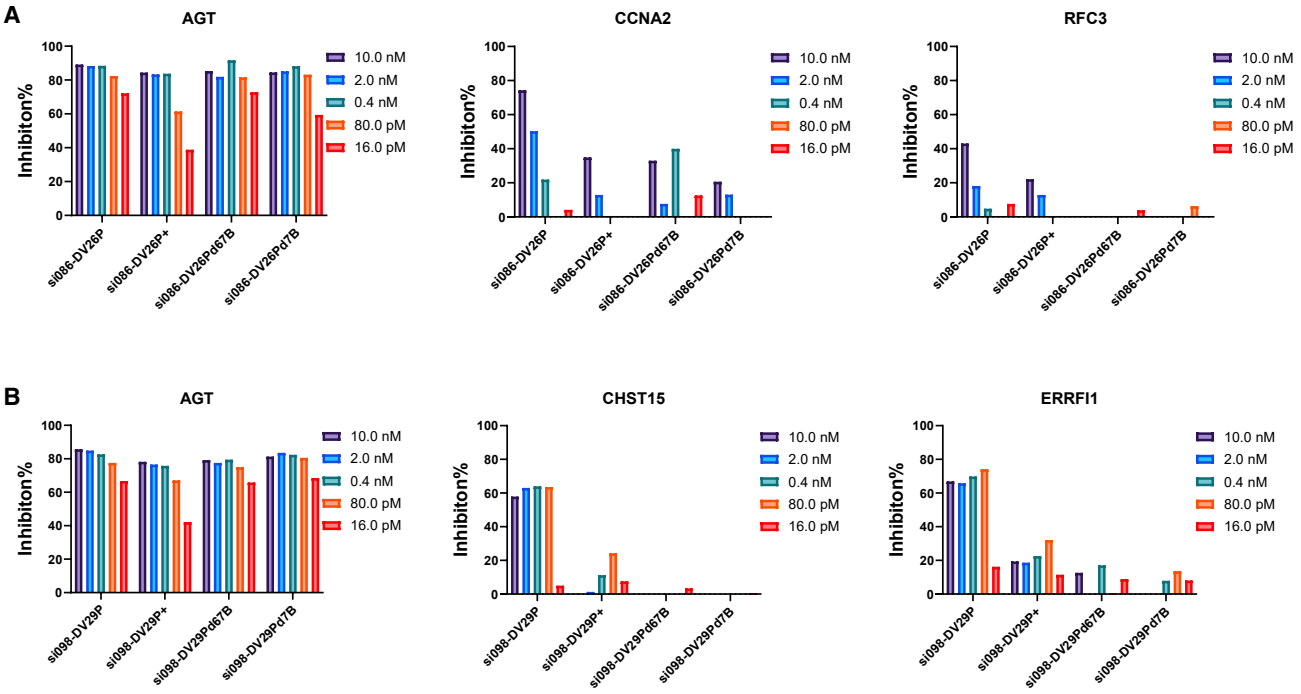

Figure 2. Off-target effects of siRNAs with DNA modifications

Inhibition of siRNAs designed based on (A) si086-DV26P and (B) si098-DV29P on off-target genes were tested in five different concentrations using qPCR. $n = 1$.

off-target genes was individually verified through in-vitro qPCR. Most candidate siRNAs exhibited little potential off-target effects on those genes (Figures S10 and S11). However, two siRNAs, si098-DV29P and si086-DV26P, exerted relatively strong inhibition on their potential off-target genes (Figures S10B and S10E), suggesting that measures should be taken to prevent and control the off-target risk.

We sought to reduce the off-target risk through chemical modifications. It is reported that the specially designed modification patterns, such as glycol nucleic acid (GNA) modification at specific positions, could reduce the off-target effects,[19,20] and such design may also help to improve the no-observed-adverse-effect level (NOAEL) of siRNAs. Inspired by the report that siRNAs with DNA substitution at the 5′ end of the antisense strand can reduce off-target effects,[21,22] we tried DNA substitutions at the specific positions of the seed region for candidate siRNAs to reduce their off-target effect. Several modification patterns with substituted nucleotides at different positions on the antisense strand were designed based on si086-DV26P. For example, DV26Pd7 was generated by replacing the 7th nucleotide on antisense strands of DV26P siRNAs with DNA. In the case of DV26Pd7B, it involved substituting the nucleotide on antisense strands as well as the complementary nucleotide on the sense strands. Their on-target and off-target effects were analyzed in HepG2 cells (Figure S12). The results indicated that si086-DV26P with modification patterns d7B and d67B, which involved DNA substitution at position 7 or position 6-7 of the antisense strand and the corresponding position on the sense strand, could reduce its off-target activity while retaining the on-target efficacy (Figure 2A). The effect of DNA substitution had a higher inhibition for target *AGT* compared to the same sequence with GNA substitution at position 6 of antisense strands (labeled with "+" at the end of the siRNA name).

These two patterns were then applied to si098-DV29P to evaluate its anti-off-target effects. Similar to the demonstration above, DNA substitution significantly reduced the off-target effects of si098-DV29P without compromising the knockdown efficiency of the *AGT* mRNA (Figure 2B). These two patterns were selected for further *in vivo* screenings.

In vivo silencing of *AGT* by GalNAc-siRNAs

Although most *in silico* predicted off-target genes showed minimal risk in qPCR validation, DV26Pd7B and DV26Pd67B modifications were introduced to 12 of the 13 potent siRNAs identified in the *in vitro* study (excluding si061-DV27P). Finally, a total of 34 GalNAc-siRNAs were designed and synthesized for subsequent *in vivo* evaluation (Figure 3A). The humanized *AGT* mice were dosed with a single subcutaneous injection (s.c., $n = 6$ per group) at a dose of 3 mg per kilogram (mpk). Serum AGT levels were determined by ELISA on days 3, 7, 14, 21, and 28 post-dosing. All siRNAs without DNA substitutions or with d7B modifications had significantly reduced plasma hAGT levels from day 7 to day 28, with a maximum reduction exceeding 80% (Figure 3A). However, all

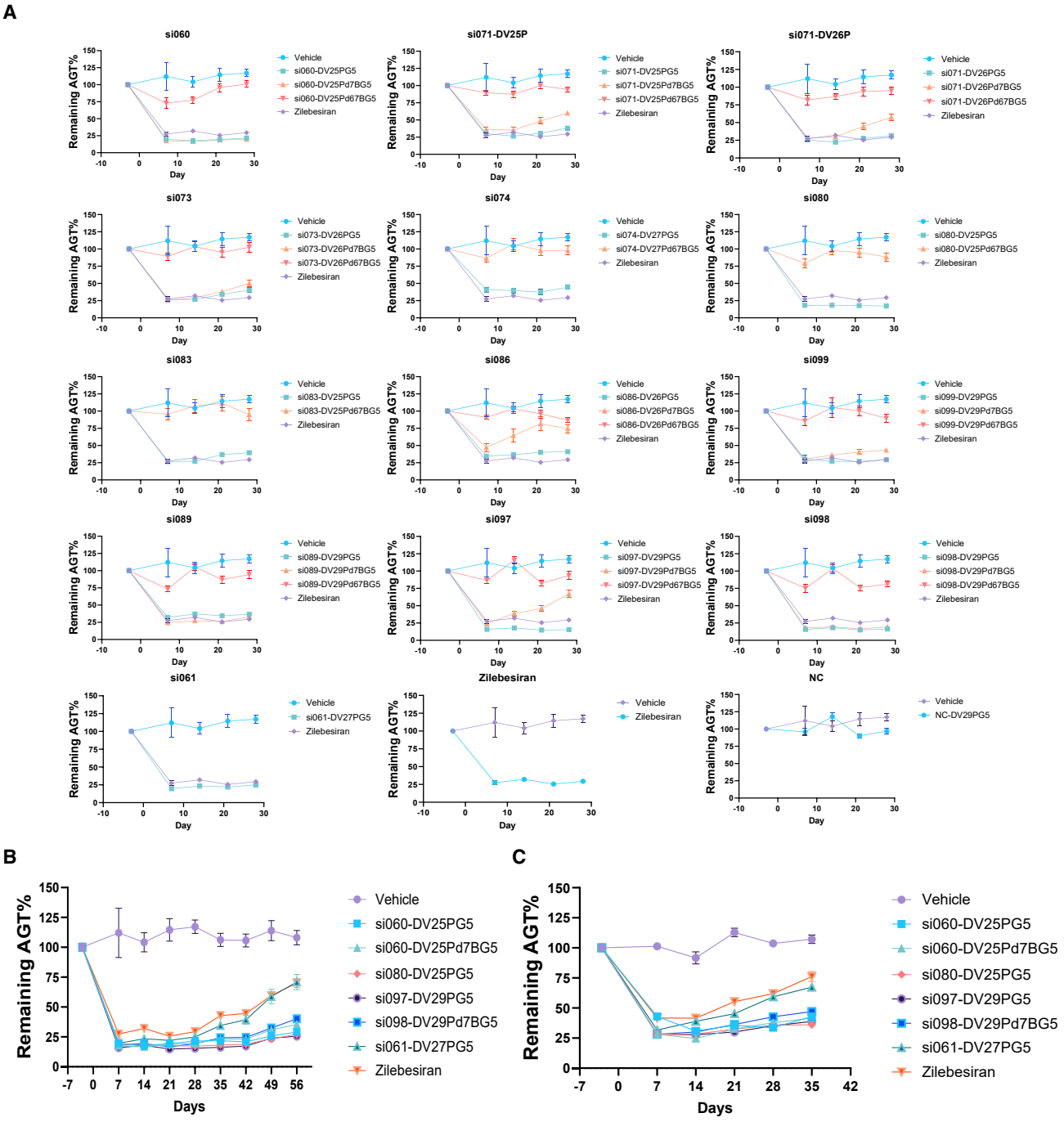

Figure 3. Selection of AGT siRNAs in human AGT transgenic mice

(A) Inhibition of serum AGT expression in mice at single dose of 3 mpk on days 7, 14, 21, 28, and 35. *n* = 6 for each group. Group means ± SEM are shown. (B) Inhibition of serum AGT expression in mice at single dose of 3 mpk from day 7 to day 56. *n* = 6 for each group. Group means ± SEM are shown. (C) Inhibition of serum AGT expression in mice at single dose of 1 mpk on days 7, 14, 21, 28, and 35. *n* = 6 for each group. Group means ± SEM are shown.

siRNAs with d67B modifications, which were effective *in vitro* screening, exhibited a significantly lower inhibitory activity *in vivo*. We hypothesized that the two consecutive DNA substitutions at the seed region of siRNAs resulted in poor resistance to nucleases in the liver or blood, ultimately reducing their *in vivo* efficacy. A pharmacokinetics test of si060-DV25PG5 and si060-DV25Pd67BG5

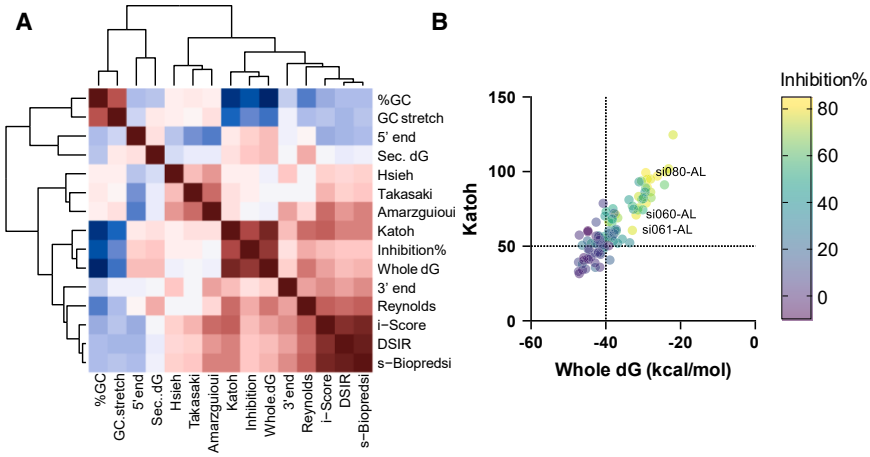

Figure 4. Features and model predictions of siRNA sequences

(A) Pearson correlation coefficient between pairs of siRNA efficacy (Inhibition%) and different features or model predictions. (B) Whole dG and Katoh values of alternately modified siRNAs presented in this study. Dots of siRNAs are colored according to their efficacy (Inhibition%). Grid lines of Whole dG = −40 kcal/mol and Katoh = 50 are shown on the graph. Corresponding alternately modified siRNAs of potent siRNAs from *in vivo* screening are labeled in the graph. si60-AL and si80-AL are labeled. si097-AL and si098-AL have similar Whole dG (−32.2 and −32.5 kcal/mol, respectively) and Katoh score (68.7 and 68.8, respectively) with si060-AL (Whole dG: −31.9 kcal/mol, Katoh score: 70.9) and locate closely to si060-AL on the graph.

in Sprague-Dawley (SD) rats was conducted to elucidate the reason for these significant pharmacological differences between *in vitro* and *in vivo* results (Figure S13). It was observed that the concentration of si060-DV25Pd67BG5 in the liver decreased faster than si060-DV25PG5, suggesting its lower stability compared to si060-DV25PG5.

The observation periods were extended to 56 days post-dosing for the six most potent candidates (Figure 3B). Serum hAGT levels in all groups reached the nadir between day 14 and day 21. Among these, in the si071-DV26PG5, si061-DV27PG5, and Zilebesiran groups, by day 56, the serum hAGT levels had rebounded successively, exceeding 50% of the inhibition rate at the nadir. In contrast, the si060-DV25PG5, si060-DV25Pd7BG5, si080-DV25PG5, si097-DV29PG5, and si098-DV29Pd7BG5 groups maintained their potency even on day 56. This indicated that they exhibited a more persistent inhibitory on serum hAGT levels compared to Zilebesiran. Mice were then sacrificed at the end of the observation period, and hepatic *hAGT* mRNA levels were analyzed by qPCR. In line with the serum hAGT reduction on day 56, 80% downregulation of liver *hAGT* mRNA level was observed in all five potent siRNAs, while the downregulation for the Zilebesiran group was only 34% (Figure S14).

To further differentiate the efficacy of the five potent siRNAs, a lower-dose study was conducted. Humanized *AGT* mice received a single subcutaneous injection of 1 mpk of each siRNA (n = 6 per group). The results confirmed that all five siRNAs exhibited comparable efficacy, significantly and sustainably reducing both serum hAGT levels and liver *hAGT* mRNA levels over a 35-day period (Figures 3C and S14). Notably, their efficacy surpassed that of Zilebesiran, demonstrating significant improvement.

Predictive effect of Gibbs free energy and Katoh score on the efficacy of alternately modified siRNAs

In silico efficacy prediction of siRNAs can be performed using a variety of algorithms based on different sets of rules.[23–25] To investigate the predictive effect of existing methods using our collected data, we compared the efficacy (Inhibition%) of alternately modified siRNAs presented in this study with scores or features calculated with existing algorithms using the i-Score tool in XLS format (Table S1).[23] The correlation coefficient was low for most algorithms except for thermodynamic features and a model proposed by Katoh et al. (Figure 4A).[26] Higher whole-sequence Gibbs free energy (Whole dG) and Katoh score are correlated with higher siRNA efficacy, with correlation coefficients of 0.805 and 0.751, respectively.

We next sought to distinguish high-efficacy siRNAs from all siRNAs based on Whole dG and Katoh scores. siRNAs with higher efficacy (dots in brighter colors) roughly have a Whole dG of over −40 kcal/mol and a Katoh score of over 50 points (Figure 4B). Potent siRNA candidates from *in vivo* screening in mice (si060-DV25PG5, si060-DV25Pd7BG5, si080-DV25PG5, si097-DV29PG5, and si098-DV29Pd7BG5) also satisfied abovementioned conditions (Table S1). These five siRNAs, together with si061-DV27PG5, were chosen for *in vivo* toxicology studies in SD rats.

Toxicology in SD rat

A 2-week repeat dose-range finding study (DRF) of si060-DV25PG5, si060-DV25Pd7BG5, si080-DV25PG5, si097-DV29PG5, si098-DV29Pd7BG5, si061-DV27PG5, and Zilebesiran in SD rats was performed, respectively. In this study, SD rats were randomly allocated into 15 groups based on body weight, 3/sex for each group. The vehicle control group was administered with 0.9% sodium chloride, and every candidate siRNA injection was separated into a low-dose (50 mpk) group and a high-dose (200 mpk) group. For every dose group, SD rats were administered via subcutaneous injection once every two weeks for two consecutive doses (two doses in total). si097s-DV29PG5, si098-DV29PG5, and Zilebesiran had no effect on blood ALT, AST, or urea levels (Figures 5A and S15). Rats were then sacrificed at the end of the study, and histopathology examinations were performed on tissues of interested groups (Figures 5B and S16–S17; Tables 1, S2, and S3). For si097-DV29PG5, histopathological findings were observed in the liver (minimal to mild vacuolation of hepatocytes, minimal apoptosis or single cell necrosis of

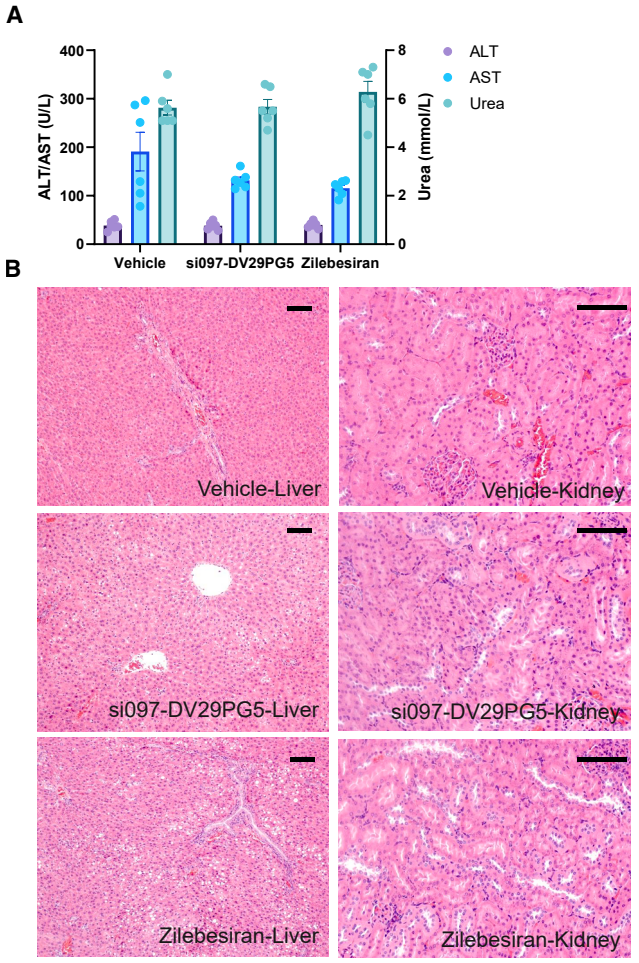

Figure 5. Toxicology tests for candidate siRNAs in rats

(A) Blood ALT, AST, and urea levels of rats administrated with candidate siRNAs. n = 6 for each group. Group means ± SEM are shown. (B) Histopathology examinations of rat livers and kidneys. Scale bar, 100 μm.

hepatocytes, minimal increased Kupffer cells, and minimal to mild basophilic granules of Kupffer cells) and kidney (minimal to moderate basophilic granules of cortical tubular epithelial cells). For Zilebesiran, similar histopathological findings were also observed in the liver (minimal to mild vacuolation of hepatocytes, mild hyalinosis of hepatocytes, and minimal apoptosis or single cell necrosis of hepatocytes) and kidney (moderate basophilic granules of cortical tubular epithelial cells). The number of animals with the mentioned histopathological findings was comparable in the si097-DV29PG5 and Zilebesiran groups. Thus, it can be concluded that si097-DV29PG5 has an equivalent safety profile to Zilebesiran.

RNAseq analysis

Previous studies have reported that rodent hepatotoxicity can largely be attributed to RNAi-mediated off-target effects.[19,20] To further assess the safety profile of candidate siRNAs, RNAseq was conducted to investigate their off-target effects in primary human and rat hepatocytes, respectively. siRNAs used in rat toxicology tests were introduced into primary human or rat hepatocytes through free uptake at different concentrations. Sequencing was performed, and differentially expressed genes (DEGs) were analyzed (Table 2). Genes whose expression decreased with elevated siRNA concentration were enriched and considered treatment-related. Treatment-related genes, that complementary pairing to the seed region of the antisense strands of siRNAs were considered sequence-related. si061-DV27PG5 has the highest number of treatment-related or sequence-related DEGs in rats, which might explain its hepatotoxicity in rats. On the other hand, si097-DV29PG5 and si098-DV29PG5 with fewer DEGs in rat hepatocytes may explain their good safety profiles in toxicology tests in rats, supporting the opinion that off-target effects may contribute to the hepatotoxicity. No sequence-related off-target genes were observed for si060-DV25pG5, si097-DV29PG5, si098-DV29Pd7BG5, si061-DV27P5, or si060-DV25Pd7BG5 in primary human hepatocytes, suggesting a better safety profile for these siRNAs in humans.

The efficacy proof of concept in spontaneous hypertensive cynomolgus monkeys

To further evaluate the blood pressure-lowering effect of candidate siRNAs, the spontaneous hypertension cynomolgus monkey model, which closely resembles primary hypertension in humans, was chosen for the test. Three optimal potent siRNAs, si097-DV29PG5, si060-DV25PG5, and si080-DV25PG5, were selected for testing and compared with Zilebesiran. Cynomolgus monkeys were dosed s.c. once (6 mpk, n = 3 per group, male). Serum AGT levels (Figures 6A and 6B) and blood pressure (Figures 6C and 6D) were measured weekly. At 6 mpk, all candidate siRNAs were able to achieve a maximum reduction in serum AGT levels by over 90%, and systolic blood pressure was also lowered by over 30 mmHg compared to baseline on day 28. Blood pressure remained around 20 mmHg below baseline on day 91 for si097-DV29PG5, indicating a strong and persistent blood-pressure-lowering effect. No significant differences were observed between different groups, suggesting equivalent inhibitory efficacy on blood pressure lowering to Zilebesiran under the dosage of 6 mpk. Furthermore, si097-DV29PG5 was selected for a low-dose test wherein the spontaneous hypertension cynomolgus monkey was administrated via s.c. once (3 mpk, n = 3 per group, male). Serum AGT levels (Figure 6B) maximally decreased 98% for si097-DV29PG5 and 96% for Zilebesiran, whereas the average blood pressure (Figure 6D) maximally decreased by 33 mmHg and 27 mmHg, respectively. The candidate si097-DV29PG5 showed a better average SBP reduction effect than Zilebesiran even to the endpoint of the experiment (22 mmHg vs. 11 mmHg on day 84). Consistent with this difference, the inhibition rate of AGT in monkey serum by si097-DV29PG5 remained 96% at the endpoint, whereas in the Zilebesiran group, a rebound of AGT inhibition rate was observed (from the highest 96% on day 21–87% on day 84). Due to the limitation of a small sample size, a significant difference has not been observed. However, the abovementioned results may still indicate the potential superiority of si097-DV29PG5 compared to Zilebesiran.

Table 1. Major microscopic pathologic changes from animals sacrificed on D23

	Males					Females				
Test articles	Saline	si097-DV29PG5		Zilebesiran		Saline	si097-DV29PG5		Zilebesiran	
Group	**1**	**2**	**3**	**14**	**15**	**1**	**2**	**3**	**14**	**15**
Dose (mpk)	**0**	**50**	**200**	**50**	**200**	**0**	**50**	**200**	**50**	**200**
Number of examined animals	**3**	**3**	**3**	**3**	**3**	**3**	**3**	**3**	**3**	**3**
Liver										
Vacuolation, hepatocytes	**1**	**1**	**1**	**1**	**2**	**3**	**2**	**3**	**0**	**3**
minimal	1	1	0	0	1	3	2	2	0	1
mild	0	0	1	1	1	0	0	1	0	1
moderate	0	0	0	0	0	0	0	0	0	1
Hyalinosis, hepatocytes	**0**	**0**	**0**	**0**	**1**	**0**	**0**	**0**	**0**	**0**
mild	0	0	0	0	1	0	0	0	0	0
Increased mitotic figures, hepatocytes	**0**	**0**	**0**	**0**	**0**	**0**	**0**	**0**	**0**	**0**
minimal	0	0	0	0	0	0	0	0	0	0
Increased Kupffer cells	**0**	**0**	**0**	**0**	**0**	**0**	**0**	**1**	**0**	**0**
minimal	0	0	0	0	0	0	0	1	0	0
Apoptosis/single cell necrosis, hepatocytes	**0**	**0**	**0**	**1**	**3**	**0**	**0**	**3**	**0**	**1**
minimal	0	0	0	1	3	0	0	3	0	1
Basophilic granules, Kupffer cells	**0**	**0**	**0**	**0**	**0**	**0**	**0**	**3**	**0**	**0**
minimal	0	0	0	0	0	0	0	2	0	0
mild	0	0	0	0	0	0	0	1	0	0
Cholestasis, Kupffer cells	**0**	**0**	**0**	**0**	**0**	**0**	**0**	**0**	**0**	**0**
minimal	0	0	0	0	0	0	0	0	0	0
Kidney										
Basophilic granules, cortical tubular epithelial cells	**0**	**3**	**3**	**0**	**3**	**0**	**3**	**3**	**3**	**3**
minimal	0	3	0	0	0	0	2	0	3	0
mild	0	0	1	0	0	0	1	0	0	0
moderate	0	0	2	0	3	0	0	3	0	3

DISCUSSION

siRNA therapeutics have emerged as a highly promising approach for treating chronic diseases associated with the overexpression of specific mRNAs, particularly following the groundbreaking success of Zilebesiran, a siRNA agent targeting *AGT* mRNA, in hypertension treatment.[9,11] However, the development of potent siRNA agents still faces many significant challenges. The absence of a precise tool for the prediction of structure-activity relationships makes it difficult to design an siRNA with satisfactory efficacy and safety. In this study, we have introduced an innovative and comprehensive drug discovery platform specifically designed to optimize the synergistic integration of sequence composition, modification patterns, and targeted delivery mechanisms.

By using this innovative platform, several novel and potent siRNAs targeting *AGT* were successfully developed. Initially, to avoid the susceptibility of naked siRNAs to ribonuclease degradation and their inherent chemical instability, alternating 2′-F/2′-MOE modifications (termed "AL") were introduced. From the initial pool of 96 siRNA sequences, 19 AL-modified sequences (Figure 1A) were selected based on their dose-dependent efficacy in HepG2 and Huh7 cells. Further evaluation had determined 10 potent AL-modified sequences (Figure 1B). Notably, the most potent sequence, si060-AL, demonstrated remarkable inhibitory activity with IC_{50} values of 2.25 pM in HepG2 cells and 2.26 pM in Huh7 cells, which is 4.4-fold and 2.9-fold better respectively over Zilebesiran-AL (with IC_{50} of 9.98 pM in HepG2 and 6.60 pM in Huh7). This significant enhancement in potency highlights the superiority of these sequences compared to Zilebesiran. Based on these results, 75 siRNAs with diverse modification patterns were designed from the 10 potent sequences and subsequently screened in both HepG2 and Huh7 cells (Figure S5).

As a result, 13 highly potent siRNAs were identified. Although eight modification patterns (Figure S1), DV25P–DV29P and

Table 2. AGT inhibition (%) and no. of DEGs in human and rat primary hepatocytes

Test articles	AGT inhibition (human)/%			No. of DEGs in human	No. of seed-region-related DEGs in human	AGT inhibition (rat)/%			No. of DEGs in rat	No. of seed-region-related DEGs in rat
	100 nM	10 nM	1 nM			100 nM	10 nM	1 nM		
Zilebesiran	67.36	51.84	31.87	159	6	−13.21	−6.39	3.32	83	4
si060-DV25Pd7BG5	73.54	53.55	25.09	22	0	−28.25	−20.35	−18.13	77	0
si097-DV29PG5	81.85	59.05	29.67	43	0	−15.66	−27.94	−25.51	6	2
si080-DV25PG5	75.08	55.77	34.61	30	6	−13.86	−20.08	−16.93	3	2
si098-DV29Pd7BG5	75.91	58.76	27.13	3	0	12.03	18.91	−15.95	6	0
si061-DV27PG5	56.38	44.80	29.29	2	0	−26.31	−32.25	−24.21	136	4
si060-DV25PG5	68.62	48.90	30.50	1	0	−14.65	−24.44	−5.31	27	0

DV32P–DV34P, were designed and screened, four of them were superior and emerged in several distinct sequences (DV25P, DV26P, DV27P, and DV29P). For instance, si89, si97, si98, and si99, with modification pattern DV29P, exhibited excellent target inhibition effects (Figures 1C and 1D). Notably, si89-DV29 had achieved IC_{50} values of 3.30 pM in HepG2 cells and 1.83 pM in Huh7 cells, which was 5.2-fold and 1.7-fold better, respectively, over Zilebesiran (17.27 pM in HepG2 and 3.09 pM in Huh7). These results highlight the enhanced efficacy of these siRNAs, which may be attributed to an optimal combination of sequence composition and modification patterns.

Furthermore, the successful transfer of effective modification patterns across different sequences suggests their broad applicability. However, modification patterns may not be universal. Despite using the DV29 pattern, si102-DV29P had shown a significantly weaker inhibition (IC_{50} values of 61.50 pM in HepG2 and 15.08 pM in Huh7). This underscores the sequence specificity of modification patterns, emphasizing the necessity of screening experiments for the identification of the most effective combinations.

Next, the potential off-target effects of siRNAs were analyzed by *in silico* analysis, leveraging insights from evaluation reports of several approved siRNAs.[27] Among the 13 potent modified siRNAs selected, 12 had exhibited potential off-target effects (Figures S10 and S11). qPCR validation in both HepG2 and Huh7 cells revealed that si86-DV26P may have a significant off-target effect on the gene CCNA2 and showed a dose-dependent inhibition at a concentration range of 16 pM to 10 nM, with a maximum inhibition of up to 80% (Figure S10F). To address this, a DNA substitution strategy was first explored, and two modified patterns, DV26Pd7B and DV26Pd67B, were applied on si86 to design two new compounds, si86-DV26Pd7B and si86-DV26Pd67B (Figure 2A). The GNA modification pattern, reported by Alnylam,[19,20] was also involved in si86-DV26P+ as a comparison.

The ideal outcome is to eliminate off-target gene inhibition without compromising on-target gene suppression. However, achieving this target can be a challenge since modifications that reduce off-target effects could also diminish on-target efficacy. Our results showed that GNA modification in si86-DV26P+ has reduced the inhibition of CCNA2 but also slightly impaired *AGT* suppression. In contrast, si86-DV26Pd7B and si86-DV26Pd67B had effectively minimized CCNA2 inhibition while maintaining robust on-target activity. Similar results were also observed for si98-DV29P (Figure 2B), confirming the efficacy of DNA substitution strategy in mitigating off-target effects. As a precaution, DV26Pd7B and DV26Pd67B modifications were applied to 11 additional siRNAs together (excluding si061-DV27P, which had no off-target genes found), resulting in the design of 34 GalNAc-siRNA conjugates for further *in vivo* evaluation (Figure 3).

During siRNA-mediated gene silencing, the RNA-induced silencing complex (RISC) demonstrates high specificity in binding target mRNA.[28] However, due to significant genetic homology differences between species, siRNAs designed for human mRNA often fail to effectively recognize their counterparts in wild-type mice. This limitation can be overcome by using humanized mouse models, which provide a suitable genetic background for successful siRNA targeting and enable effective translation of pharmacodynamic profiles to humans.[29]

In this study, we utilized humanized *AGT* mice for *in vivo* screening to evaluate the efficacy of GalNAc-siRNA conjugates. Following a single subcutaneous injection of siRNAs at 3 mpk, we identified 6 out of 34 conjugates that showed equivalent or superior efficacy compared to Zilebesiran (Figures 3A and 3B). While the nadir AGT levels of these potent siRNAs and Zilebesiran were comparable at both 3 mpk and 1 mpk doses, significant differences between candidate siRNAs and Zilebesiran were observed during the rebound phase, revealing distinct long-term performance profiles among the candidates (Figures 3B and 3C). Notably, si097-DV29PG5 outperformed Zilebesiran in both AGT inhibition and duration of effect *in vivo*. This finding aligned with the *in vitro* results, where the non-GalNAc-conjugated counterpart, si097-DV29, also demonstrated superior efficacy over Zilebesiran (Figure 1D). However, promising *in vitro* results may not always be reserved *in vivo* due to the complexity of siRNA delivery. For instance, although siRNAs with d67B modification (has DNA substitutions at positions 6 and 7 of the antisense strand) had achieved a favorable balance

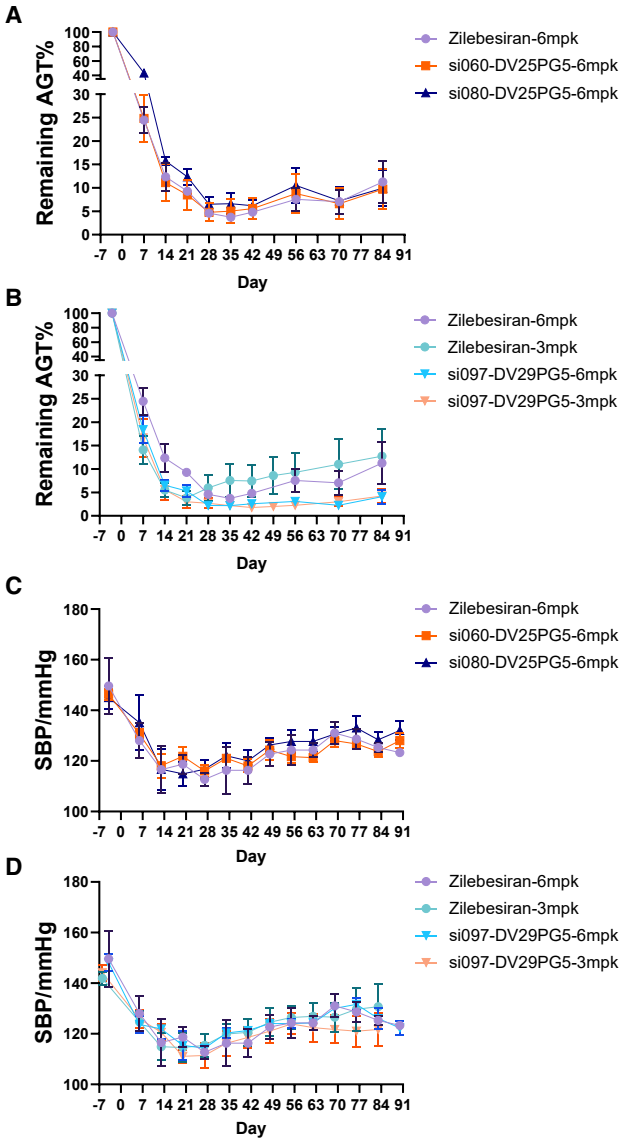

Figure 6. AGT inhibition and blood-pressure-lowering effects of candidate siRNAs in cynomolgus monkeys

(A) and (B) Systolic blood pressure of subject monkeys. $n = 3$ for each group. Group means ± SEM are shown. (C) and (D) Serum AGT expression of monkeys treated with candidate siRNAs by 6 mpk s.c. $n = 3$ for each group. Group means ± SEM are shown.

between off-target and on-target effects *in vitro*, rapid clearance of these siRNAs from tissues had resulted in poor *in vivo* efficacies (Figures 3A, S12, and S13). In summary, mitigating off-target effects through siRNA modifications remains a significant challenge and requires thorough validation in both *in vitro* and *in vivo* settings.

With the abundant pharmacodynamic profile of siRNAs in hand, we aimed to establish a prediction model to elucidate the relationship between the sequence composition and efficacy. Given that the *AGT* mRNA exceeds 2,000 nt in length, thousands of siRNAs with diverse sequence compositions can be designed. While *in silico* efficacy prediction of siRNAs can be performed using various algorithms based on different rule sets,[23–25] most existing models have shown low correlation coefficients when applied to alternately modified siRNAs in this study when evaluated using the i-Score tool (Figure 4).[23] Notably, thermodynamic features and the model proposed by Katoh et al.. were exceptions,[26] as we have demonstrated that higher whole-sequence Gibbs free energy (Whole dG) and Katoh score correlated with increased *in vitro* siRNA efficacy. Thermodynamic features were known to influence siRNA efficacy,[30–32] and the Katoh score, derived from siRNA base composition, could also impact inhibitory.[26] The failure of other features, rule sets, or models to predict the efficacy of alternately modified siRNAs likely stems from their reliance on datasets of unmodified siRNAs,[14] which are less effective for modified sequences. Additionally, unmodified siRNAs possess some disadvantages compared to fully modified siRNAs[13] and thus might be influenced by different parameters. Currently, few models are trained on data from modified siRNAs, underscoring the continued necessity of *in vitro* or *in vivo* screening to identify potent sequences.

Beyond pharmacodynamic considerations, safety profiles are equally critical for the development of therapeutic siRNAs. To assess the safety of six candidate compounds identified in the pharmacodynamic study using humanized *AGT* mice, *in vivo* toxicology tests were conducted in SD rats (Tables S2 and S3). While si097-DV29PG5 had demonstrated safety (Figure 5; Table 1), although some "safe" siRNAs, particularly si061-DV27PG5, still induced liver or kidney damage (Figures S14–S17). Despite having the lowest number of predicted off-target genes, si061-DV27PG5 caused the most significant adverse effects, including elevated ALT, AST, and urea levels, as well as histopathological liver and renal damage. Hepatotoxicity in rats is primarily driven by RNAi-mediated off-target effects, and strategies to reduce seed-mediated off-target binding could improve the safety of GalNAc-siRNA therapeutics.[19] Although *in silico* analysis is widely used for off-target risk assessment, our findings align with recent reports demonstrating that many predicted off-target genes may not be accurate when validated by qPCR. Given the complexities of predicting the off-target effect of siRNA, even with perfect sequence matches, it is unsurprising that most candidate siRNAs exhibited no inhibitory effects on predicted off-target genes.

To further investigate, we employed RNAseq to comprehensively evaluate the off-target effects of siRNAs for toxicology studies. Differentially regulated genes were selected based on the assumption that siRNA-mediated gene regulation should follow dose-dependent patterns (Table 2). Among the tested siRNAs, si061-DV27PG5 induced the highest number of downregulated genes in rat hepatocytes, a finding that strongly correlated with toxicology test results. However, the discrepancy between the number of downregulated genes and off-target genes predicted using NCBI blast raised questions regarding the extent to which these genes were affected by miRNA-like off-target mechanisms. To answer this question, we

utilized DSIR to identify genes with a 3′UTR sequence complementary to the siRNA seed region. The results revealed that less than 5% of these genes were dose-dependently downregulated by siRNA, underscoring the significant challenges in the accurate prediction of off-target effects. Together, these findings highlight the need for more robust predictive models to improve the *in silico* forecasting of off-target effects of siRNAs.

Based on their comparable efficacy in humanized *AGT* mice and favorable safety profiles, three potent siRNAs—si60-DV25PG5, si80-DV25PG5, and si097-DV29PG5—were selected for further validation in spontaneous hypertensive monkeys (Figure 6). Single subcutaneous injections of the respective siRNAs were given to animals. Both si60-DV25PG5 and si80-DV25PG5 demonstrated comparable efficacy in AGT inhibition and systolic blood pressure (SBP) reduction to Zilebesiran (Figures 6A and 6C). Notably, si097-DV29PG5 had achieved >90% reduction in serum AGT levels, regardless of the administered dose (6 mpk and 3 mpk) (Figure 6B). This may suggests a saturation of siRNA activity at 3 mpk. Importantly, si097-DV29PG5 maintained sustained AGT inhibition throughout the observation period, whereas Zilebesiran had exhibited a marked rebound trend. Despite these differences in AGT suppression, both siRNAs had demonstrated comparable blood pressure reduction, indicating that the achieved AGT knockdown levels may be sufficient to sustain the antihypertensive effect in the cynomolgus monkeys. Given its prolonged maximal AGT suppression, si097-DV29PG5 holds significant potential to be a superior antihypertensive therapy compared to Zilebesiran, particularly at equivalent or lower doses.

In conclusion, this study established a comprehensive framework for therapeutic siRNAs development, integrating efficacy and safety considerations. We successfully developed a novel siRNA, si097-DV29PG5, targeting hepatic AGT for hypertension treatment. Compared to Zilebesiran, a phase II clinical trial candidate, si097-DV29PG5 exhibited superior efficacy and prolonged duration of effect, positioning it as a promising solution for uncontrolled hypertension. Throughout development, we have fully considered both high efficacy and rigorous safety evaluation, ultimately identifying si097-DV29PG5 as a potent and safe *AGT*-targeting siRNA. However, its clinical safety and efficacy require further validation. The systematic approach established in this study can be extended to other siRNA-based therapies, providing a versatile blueprint for therapeutic discovery.

MATERIALS AND METHODS

Care and use of laboratory animals

All studies were conducted using protocols consistent with applicable local regulations and were approved by the Institutional Animal Care and Use Committee (IACUC, IACUC20231113-PD02.01). The test articles were diluted with 0.9% NaCl or PBS to achieve appropriate dosing concentrations and were administered subcutaneously to C57/BL6 mice (6–8 weeks old), Sprague-Dawley rats (6–8 weeks old), or cynomolgus monkeys (6–14 years old). Randomization was performed to avoid bias. Investigators were not blinded to the group allocation during the experiment or when assessing the outcome.

siRNA design and synthesis

siRNAs targeting *AGT* were designed based on mRNA sequence NM_001384479.1 obtained from NCBI. All possible siRNA sequences were generated, and sequences with immunostimulatory motifs were filtered with DSIR.[25] The sequence and modification of Zilebesiran were collected from whom INN recommended list 86 (https://www.who.int/publications/m/item/inn-rl-86). The efficacy of sequences was predicted using different rule sets or models,[25,26,33,34] then sequences used in screening were picked manually. We alternately modified siRNAs with 2′-F and 2′-MOE for sequence composition screening. We managed to identify several siRNAs with different sequence compositions, most of which were more potent compared with Zilebesiran congener, which also had the same alternative modification as all the candidates. Then different modification patterns were applied on siRNAs for modification screening.

The fully protected single strands of the siRNA were synthesized using a Tsingke 192P or 12P synthesizer. Nucleotide phosphoramidite of 2′-F, 2′-Ome, DNA, and GNA were obtained from commercial sources. GalNAc G5 was synthesized and then attached to the controlled pore glass (CPG) solid-phase support. The 5′ end of GalNAc G5 was protected by 4,4′-dimethoxytrityl (DMT). This protecting group can be removed at the start of nucleotide assembly, allowing GalNAc G5 to conjugate with the 3′ end of the sense strand during solid-phase synthesis. After the solid-phase synthesis was completed, the antisense strand and sense strand were separately cleaved from the synthesis support. This cleavage was achieved by subjecting them to a 28% ammonia solution at 85°C for a duration of 2 h. After that, the system was cooled to room temperature. The mixture was then transferred to a filter press and eluted with a mixed solution of purified water and ethanol. The filtrates were combined, passed through a chromatography column, desalted, and concentrated using a 1 KD ultrafiltration tube to obtain a single-strand solution. The purified sense and antisense strands were mixed in a 1:1 ratio, heated to 95°C and held at this temperature for 3 min, and then slowly cooled to room temperature to form double-stranded siRNA. After lyophilization, the siRNA was obtained as a white powder. The identities and purities of all oligonucleotides were confirmed using LC-MS and HPLC, respectively. Before testing *in vitro* or administration to the animals, the oligonucleotide solution was prepared to a certain concentration using PBS buffer.

Cell line culture and dosing

HepG2 (Cyagene, H1-1701) and Huh7 (NIFDC, DR-Cell-01) cells were grown in Dulbecco's modified Eagle's medium (Macgene, CM10013) supplemented with 5% fetal bovine serum (FBS; Vistech, SE100-011) and 1% penicillin-streptomycin (Gibco, 15070063). Reverse transfections were performed in a 24-well plate using Lipofectamine RNAiMAX (Invitrogen, 13778150), according to the

manufacturer's instructions. Briefly, test articles were dissolved in water, diluted using Opti-MEM (Gibco, 31985070), and mixed with an equal volume of Lipofectamine RNAiMAX dispersed in Opti-MEM. The mixture was incubated for 15 min at room temperature to form siRNA-Lipofectamine RNAiMAX transfection complexes. Cells were detached and diluted in Opti-MEM such that 500 μL contains 75,000 cells. One hundred microliters of transfection complexes were added to each well, and 500 μL of diluted cells were added to a final volume of 600 μL. The plates were gently mixed by rocking them back and forth.

Analysis of *hAGT* knockdown in transgenic mice

Male *hAGT* transgenic mice were dosed with 3 mg/kg (mpk) or 1 mpk GalNAc-siRNAs via subcutaneous injection at a dose volume of 5 mL/kg (n = 6 animals per group); 0.15 mL blood sample was collected from each mouse 3 days before dosing and every 7 days after dosing. Blood samples were centrifuged at 3,000 rpm at 4°C to separate plasma, and hAGT levels in serum were determined using ELISA (Sino Biological, KIT10994). Mice were sacrificed at the end of the observation period, and their livers were collected and lysed in TRIzol (Invitrogen, 15596018CN). RNA was extracted and used for cDNA synthesis using PrimeScript RT Master Mix (Takara, RR036B), and then *hAGT* mRNA levels in the liver were determined by quantitative real-time PCR using TB Green Premix Ex Taq (Takara, RR420L) on ABI 7500 according to the manufacturer's instructions.

RNAseq

Primary human hepatocytes (Liver Biotechnology, LV-PHH001) and rat hepatocytes (Milestone Biotechnologies, CRH-100SDP-PQ) were thawed in a water bath at 37°C. Resuscitation medium was added, and the cell suspension was centrifuged at 50 ×g for 2 min. The supernatant was removed, seeding medium was added, and cells were gently resuspended. The cells were seeded in 24-well, collagen-coated plates and cultured for 24 h. siRNAs were diluted to 100 nM, 10 nM, or 1 nM with maintenance culture medium. The seeding medium was then replaced with siRNA solution, and hepatocytes were cultured for 48 h before being harvested with TRIzol (Invitrogen, 15596018CN). RNA extracted from TRIzol was used for cDNA library preparation using the Hieff mRNA Library Prep Kit (Yeasen, 12309ES08) and sequenced on a HiSeq sequencer (Illumina), according to the manufacturer's instructions. Raw RNA-seq reads were trimmed and filtered using Trimmomatic software. Filtered reads were aligned to human or rat genomes using HISAT2, and expression was quantified using StringTie. Differentially expressed genes were analyzed using DESeq.

Clinical pathology

Whole-venous blood was collected into serum separator tubes (BD Microtainer). Serum chemistry was analyzed using an AU5800 chemistry analyzer (Beckman Coulter), with reagents provided by Beckman Coulter. Blood cell counting was performed using a Sysmex XN 1,000V hematology analyzer, and blood coagulation characteristics were analyzed on a Sysmex CS-5100. Differences between group means were evaluated for statistical significance using one-way analysis of variance (ANOVA) in GNU PSPP.

Histopathology

All animals were sacrificed according to the standard operating procedures, and tissues of interest were collected. All tissues were fixed in 10% neutral buffered formalin (10% NBF) for 72 h. Tissues were trimmed, embedded in paraffin blocks, sectioned at 4 μm, stained with H&E using TissueTek Prisma A1D (Sakura), and coverslipped using TissueTek Glass g2 (Sakura). Two sections were examined microscopically from each liver in an unblinded fashion, followed by a blinded assessment to confirm subtle findings. The range of severity grade for each histologic finding was graded on a scale of 1–5, with 1 indicating minimal severity and 5 indicating severe severity.

Analysis of AGT knockdown and blood-pressure-lowering effects in spontaneous hypertensive cynomolgus monkeys

The blood pressure of 6- to 14-year-old male cynomolgus monkeys was monitored using blood pressure monitors with a cuff, and monkeys with systolic blood pressure over 140 mmHg in two consecutive measurements were considered spontaneously hypertensive animals and included in the test. The animals were randomized and allocated to different groups (n = 6 per group) based on systolic blood pressure and body weight to avoid bias. All animals were dosed with 6 mpk GalNAc-siRNAs. Blood pressure was monitored, and blood samples were collected every 7 days. Serum AGT levels were determined using ELISA.

qPCR

For cell line samples, total RNA was extracted using the MiniBest Universal RNA Extraction Kit (Takara, 9767). For animal tissue samples, total RNA was extracted using TRIzol (Invitrogen, 15596018CN) following the manufacturer's instructions. RNA was reverse-transcribed using PrimeScript RT Master Mix (Takara, RR036B). qPCR was performed with TB Green Premix Ex Taq (Takara, RR420L) according to the manufacturer's instructions on ABI 7500 using following primers: hAGT-F: 5′-ACTATCTCCCCG GACCATCC-3′, hAGT-R: 5′-CCTGATGCGGTCATTGCTCA-3′, hGAPDH-F: 5′-AGTATGACAACAGCCTCAAG-3′, hGAPDH-R: 5′-TCATGAGTCCTTCCACGATA-3′, mGAPDH-F: 5′-CCTCGT CCCGTAGACAAAATG-3′, mGAPDH-R: 5′-TTGACTGTGCCGT TGAATTTG-3′. Data were analyzed using ΔΔCt normalized to the control group (cells treated with Lipofectamin RNAiMAX alone or animals treated with PBS).

DATA AVAILABILITY

The data discussed in this publication have been deposited in NCBI's Gene Expression Omnibus[35] and is accessible through GEO Series accession number GSE291523 (https://www.ncbi.nlm.nih.gov/geo/query/acc.cgi?acc=GSE291523).

ACKNOWLEDGMENTS

We especially appreciated Mr Wei-Shi Yu, a respectable wise senior in his 80s, as the president of Youcare Pharmaceutical Group; he had given all his supports together with valuable comments for this project. We thank our colleagues from the Toxicology

group who provided insight and expertise that greatly assisted the research. We thank the colleagues of the Chemical Synthesis group for the providing of siRNAs involved in this study, and colleagues from the Pharmacology group for their efforts on the arrangements of *in vivo* experiments. We would like to acknowledge the funding from Youcare Pharmaceutical Group.

AUTHOR CONTRIBUTIONS

G.-S.S. and Z.-A.H. conceived and designed the study and revised the manuscript. Z.-A.H., G.-S.J., and S.Y. performed all the experiments and analyzed all the data. S.Y. designed siRNA sequences and modification patterns. Y.Y. was very helpful in the *in vitro* experiment. Y.-C.W. and Z.-K.T. performed all chemistry syntheses. G.-S.S. supervised the project. Z.-A.H. and G.-S.J. wrote the manuscript with input from all authors. All authors contributed to the scientific discussion and modified the manuscript. Z.-A.H., G.-S.J., and S.Y. contributed equally.

DECLARATION OF INTERESTS

All authors were employees of Beijing Youcare Kechuang Pharmaceutical Technology Co., Ltd. during the time this work was conducted.

SUPPLEMENTAL INFORMATION

Supplemental information can be found online at https://doi.org/10.1016/j.omtn.2025.102542.

REFERENCES

1. Zhou, B., Carrillo-Larco, R.M., Danaei, G., Riley, L.M., Paciorek, C.J., Stevens, G.A., Gregg, E.W., Bennett, J.E., Solomon, B., Singleton, R.K., et al. (2021). Worldwide trends in hypertension prevalence and progress in treatment and control from 1990 to 2019: a pooled analysis of 1201 population-representative studies with 104 million participants. Lancet *398*, 957–980. https://doi.org/10.1016/s0140-6736(21)01330-1.

2. Murray, C.J.L., Aravkin, A.Y., Zheng, P., Abbafati, C., Abbas, K.M., Abbasi-Kangevari, M., Abd-Allah, F., Abdelalim, A., Abdollahi, M., Abdollahpour, I., et al. (2020). Global burden of 87 risk factors in 204 countries and territories, 1990-2019: a systematic analysis for the Global Burden of Disease Study 2019. Lancet *396*, 1223–1249. https://doi.org/10.1016/s0140-6736(20)30752-2.

3. Gupta, P., Patel, P., Štrauch, B., Lai, F.Y., Akbarov, A., Marešová, V., White, C.M.J., Petrák, O., Gulsin, G.S., Patel, V., et al. (2017). Risk Factors for Nonadherence to Antihypertensive Treatment. Hypertension *69*, 1113–1120. https://doi.org/10.1161/hypertensionaha.116.08729.

4. Mooser, V., Nussberger, J., Juillerat, L., Burnier, M., Waeber, B., Bidiville, J., Pauly, N., and Brunner, H.R. (1990). Reactive hyperreninemia is a major determinant of plasma angiotensin II during ACE inhibition. J. Cardiovasc. Pharmacol. *15*, 276–282. https://doi.org/10.1097/00005344-199002000-00015.

5. van den Meiracker, A.H., Admiraal, P.J., Janssen, J.A., Kroodsma, J.M., de Ronde, W. A., Boomsma, F., Sissmann, J., Blankestijn, P.J., Mulder, P.G., Man In 't Veld, A.J., et al. (1995). Hemodynamic and biochemical effects of the AT1 receptor antagonist irbesartan in hypertension. Hypertension *25*, 22–29. https://doi.org/10.1161/01.hyp.25.1.22.

6. Sealey, J.E., and Laragh, J.H. (2007). Aliskiren, the first renin inhibitor for treating hypertension: reactive renin secretion may limit its effectiveness. Am. J. Hypertens. *20*, 587–597. https://doi.org/10.1016/j.amjhyper.2007.04.001.

7. Corvol, P., Soubrier, F., and Jeunemaitre, X. (1997). Molecular genetics of the renin-angiotensin-aldosterone system in human hypertension. Pathol. Biol. *45*, 229–239.

8. Mullick, A.E., Yeh, S.T., Graham, M.J., Engelhardt, J.A., Prakash, T.P., and Crooke, R.M. (2017). Blood Pressure Lowering and Safety Improvements With Liver Angiotensinogen Inhibition in Models of Hypertension and Kidney Injury. Hypertension *70*, 566–576. https://doi.org/10.1161/hypertensionaha.117.09755.

9. Uijl, E., Mirabito Colafella, K.M., Sun, Y., Ren, L., van Veghel, R., Garrelds, I.M., de Vries, R., Poglitsch, M., Zlatev, I., Kim, J.B., et al. (2019). Strong and Sustained Antihypertensive Effect of Small Interfering RNA Targeting Liver Angiotensinogen. Hypertension *73*, 1249–1257. https://doi.org/10.1161/hypertensionaha.119.12703.

10. Bakris, G.L., Saxena, M., Gupta, A., Chalhoub, F., Lee, J., Stiglitz, D., Makarova, N., Goyal, N., Guo, W., Zappe, D., et al. (2024). RNA Interference With Zilebesiran for Mild to Moderate Hypertension: The KARDIA-1 Randomized Clinical Trial. JAMA *331*, 740–749. https://doi.org/10.1001/jama.2024.0728.

11. Desai, A.S., Webb, D.J., Taubel, J., Casey, S., Cheng, Y., Robbie, G.J., Foster, D., Huang, S.A., Rhyee, S., Sweetser, M.T., and Bakris, G.L. (2023). Zilebesiran, an RNA Interference Therapeutic Agent for Hypertension. N. Engl. J. Med. *389*, 228–238. https://doi.org/10.1056/NEJMoa2208391.

12. Olearczyk, J., Gao, S., Eybye, M., Yendluri, S., Andrews, L., Bartz, S., Cully, D., and Tadin-Strapps, M. (2014). Targeting of hepatic angiotensinogen using chemically modified siRNAs results in significant and sustained blood pressure lowering in a rat model of hypertension. Hypertens. Res. *37*, 405–412. https://doi.org/10.1038/hr.2013.155.

13. Hu, B., Zhong, L., Weng, Y., Peng, L., Huang, Y., Zhao, Y., and Liang, X.J. (2020). Therapeutic siRNA: state of the art. Signal Transduct. Target. Ther. *5*, 101. https://doi.org/10.1038/s41392-020-0207-x.

14. Liu, B., Yuan, Y., Pan, X., Shen, H.-B., and Jin, C. (2024). AttSiOff: a self-attention-based approach on siRNA design with inhibition and off-target effect prediction. Med-X *2*, 5. https://doi.org/10.1007/s44258-024-00019-1.

15. Sliedregt, L.A., Rensen, P.C., Rump, E.T., van Santbrink, P.J., Bijsterbosch, M.K., Valentijn, A.R., van der Marel, G.A., van Boom, J.H., van Berkel, T.J., and Biessen, E.A. (1999). Design and synthesis of novel amphiphilic dendritic galactosides for selective targeting of liposomes to the hepatic asialoglycoprotein receptor. J. Med. Chem. *42*, 609–618. https://doi.org/10.1021/jm981078h.

16. Prakash, T.P., Yu, J., Migawa, M.T., Kinberger, G.A., Wan, W.B., Østergaard, M.E., Carty, R.L., Vasquez, G., Low, A., Chappell, A., et al. (2016). Comprehensive Structure-Activity Relationship of Triantennary N-Acetylgalactosamine Conjugated Antisense Oligonucleotides for Targeted Delivery to Hepatocytes. J. Med. Chem. *59*, 2718–2733. https://doi.org/10.1021/acs.jmedchem.5b01948.

17. Sebestyén, M.G., Wong, S.C., Trubetskoy, V., Lewis, D.L., and Wooddell, C.I. (2015). Targeted in vivo delivery of siRNA and an endosome-releasing agent to hepatocytes. Methods Mol. Biol. *1218*, 163–186. https://doi.org/10.1007/978-1-4939-1538-5_10.

18. Haraszti, R.A., Roux, L., Coles, A.H., Turanov, A.A., Alterman, J.F., Echeverria, D., Godinho, B.M.D.C., Aronin, N., and Khvorova, A. (2017). 5′-Vinylphosphonate improves tissue accumulation and efficacy of conjugated siRNAs in vivo. Nucleic Acids Res. *45*, 7581–7592. https://doi.org/10.1093/nar/gkx507.

19. Janas, M.M., Schlegel, M.K., Harbison, C.E., Yilmaz, V.O., Jiang, Y., Parmar, R., Zlatev, I., Castoreno, A., Xu, H., Shulga-Morskaya, S., et al. (2018). Selection of GalNAc-conjugated siRNAs with limited off-target-driven rat hepatotoxicity. Nat. Commun. *9*, 723. https://doi.org/10.1038/s41467-018-02989-4.

20. Schlegel, M.K., Janas, M.M., Jiang, Y., Barry, J.D., Davis, W., Agarwal, S., Berman, D., Brown, C.R., Castoreno, A., LeBlanc, S., et al. (2022). From bench to bedside: Improving the clinical safety of GalNAc–siRNA conjugates using seed-pairing destabilization. Nucleic Acids Res. *50*, 6656–6670. https://doi.org/10.1093/nar/gkac539.

21. Ui-Tei, K., Naito, Y., Zenno, S., Nishi, K., Yamato, K., Takahashi, F., Juni, A., and Saigo, K. (2008). Functional dissection of siRNA sequence by systematic DNA substitution: modified siRNA with a DNA seed arm is a powerful tool for mammalian gene silencing with significantly reduced off-target effect. Nucleic Acids Res. *36*, 2136–2151. https://doi.org/10.1093/nar/gkn042.

22. Ui-Tei, K., Zenno, S., Naito, Y., Takahashi, F., Nishi, K., Juni, A., Tanaka, A., and Saigo, K. (2008). DNA-modified siRNA-dependent gene silencing with reduced off-target effect is induced through a pathway parallel to that for siRNA-mediated RNA interference. In 2008 International Symposium on Micro-NanoMechatronics and Human Science (IEEE), pp. 339–345, https://dx.doi.org/10.1109/MHS.2008.4752474.

23. Ichihara, M., Murakumo, Y., Masuda, A., Matsuura, T., Asai, N., Jijiwa, M., Ishida, M., Shinmi, J., Yatsuya, H., Qiao, S., et al. (2007). Thermodynamic instability of siRNA duplex is a prerequisite for dependable prediction of siRNA activities. Nucleic Acids Res. *35*, e123. https://doi.org/10.1093/nar/gkm699.

24. Huesken, D., Lange, J., Mickanin, C., Weiler, J., Asselbergs, F., Warner, J., Meloon, B., Engel, S., Rosenberg, A., Cohen, D., et al. (2005). Design of a genome-wide siRNA library using an artificial neural network. Nat. Biotechnol. *23*, 995–1001. https://doi.org/10.1038/nbt1118.

25. Vert, J.-P., Foveau, N., Lajaunie, C., and Vandenbrouck, Y. (2006). An accurate and interpretable model for siRNA efficacy prediction. BMC Bioinf. *7*, 520. https://doi.org/10.1186/1471-2105-7-520.

26. Katoh, T., and Suzuki, T. (2007). Specific residues at every third position of siRNA shape its efficient RNAi activity. Nucleic Acids Res. *35*, e27. https://doi.org/10.1093/nar/gkl1120.

27. Friedrich, M., and Aigner, A. (2022). Therapeutic siRNA: State-of-the-Art and Future Perspectives. BioDrugs *36*, 549–571. https://doi.org/10.1007/s40259-022-00549-3.

28. Rao, D.D., Vorhies, J.S., Senzer, N., and Nemunaitis, J. (2009). siRNA vs. shRNA: Similarities and differences. Adv. Drug Deliv. Rev. *61*, 746–759. https://doi.org/10.1016/j.addr.2009.04.004.

29. McDougall, R., Ramsden, D., Agarwal, S., Agarwal, S., Aluri, K., Arciprete, M., Brown, C., Castellanos-Rizaldos, E., Charisse, K., Chong, S., et al. (2022). The Nonclinical Disposition and Pharmacokinetic/Pharmacodynamic Properties of N-Acetylgalactosamine-Conjugated Small Interfering RNA Are Highly Predictable and Build Confidence in Translation to Human. Drug Metab Dispos *50*, 781–797. https://doi.org/10.1124/dmd.121.000428.

30. Kobayashi, Y., Tian, S., and Ui-Tei, K. (2022). The siRNA Off-Target Effect Is Determined by Base-Pairing Stabilities of Two Different Regions with Opposite Effects. Genes *13*, 319. https://doi.org/10.3390/genes13020319.

31. Shabalina, S.A., Spiridonov, A.N., and Ogurtsov, A.Y. (2006). Computational models with thermodynamic and composition features improve siRNA design. BMC Bioinf. *7*, 65. https://doi.org/10.1186/1471-2105-7-65.

32. He, F., Han, Y., Gong, J., Song, J., Wang, H., and Li, Y. (2017). Predicting siRNA efficacy based on multiple selective siRNA representations and their combination at score level. Sci. Rep. *7*, 44836. https://doi.org/10.1038/srep44836.

33. Ui-Tei, K., Naito, Y., Takahashi, F., Haraguchi, T., Ohki-Hamazaki, H., Juni, A., Ueda, R., and Saigo, K. (2004). Guidelines for the selection of highly effective siRNA sequences for mammalian and chick RNA interference. Nucleic Acids Res. *32*, 936–948. https://doi.org/10.1093/nar/gkh247.

34. Reynolds, A., Leake, D., Boese, Q., Scaringe, S., Marshall, W.S., and Khvorova, A. (2004). Rational siRNA design for RNA interference. Nat. Biotechnol. *22*, 326–330. https://doi.org/10.1038/nbt936.

35. Edgar, R., Domrachev, M., and Lash, A.E. (2002). Gene Expression Omnibus: NCBI gene expression and hybridization array data repository. Nucleic Acids Res. *30*, 207–210. https://doi.org/10.1093/nar/30.1.207.